

## THE COSMIC BATTERY IN ASTROPHYSICAL ACCRETION DISKS

IOANNIS CONTOPOULOS<sup>1,\*</sup>, ANTONIOS NATHANAIL<sup>1,2</sup> AND MATTHAIOS KATSANIKAS<sup>1</sup><sup>1</sup> Research Center for Astronomy and Applied Mathematics, Academy of Athens, Athens 11527, Greece  
and<sup>2</sup>Section of Astrophysics, Astronomy and Mechanics, Department of Physics, University of Athens,  
Panepistimiopolis Zografos, Athens 15783, Greece*Draft version July 2, 2018*

## ABSTRACT

The aberrated radiation pressure at the inner edge of the accretion disk around an astrophysical black hole imparts a relative azimuthal velocity on the electrons with respect to the ions which gives rise to a ring electric current that generates large scale poloidal magnetic field loops. This is the Cosmic Battery established by Contopoulos and Kazanas in 1998. In the present work we perform realistic numerical simulations of this important astrophysical mechanism in advection-dominated accretion flows-ADAF. We confirm the original prediction that the inner parts of the loops are continuously advected toward the central black hole and contribute to the growth of the large scale magnetic field, whereas the outer parts of the loops are continuously diffusing outward through the turbulent accretion flow. This process of inward advection of the axial field and outward diffusion of the return field proceeds all the way to equipartition, thus generating astrophysically significant magnetic fields on astrophysically relevant timescales. We confirm that there exists a critical value of the magnetic Prandtl number between unity and 10 in the outer disk above which the Cosmic Battery mechanism is suppressed.

*Keywords:* Accretion; Magnetic fields

## 1. INTRODUCTION

The origin of astrophysical magnetic fields remains an open issue of modern astrophysics. Ludwig Biermann, in his famous paper, proposed a mechanism for the generation of large-scale electric currents based on the thermoelectric effect (Biermann 1950). This mechanism leads to magnetic fields that are usually quite weak initially and require subsequent dynamo amplification to reach astrophysically relevant magnitudes. Some years ago we proposed a mechanism alternative to that of the Biermann Battery (Contopoulos & Kazanas 1998, hereafter CK, Contopoulos et al. 2006), the so called Cosmic Battery. We posited that the aberration of the radiation field experienced by the electrons of an accretion flow around an astrophysical source (a generalization of the well known Poynting-Robertson effect; Poynting 1903, Robertson 1937, Lamb & Miller 1995, Bini et al. 2009, Koutsantoniou & Contopoulos 2014) generates toroidal electric currents sufficiently large to support poloidal magnetic fields that under certain astrophysically plausible circumstances will grow to equipartition values. The aberrated radiation force implies a direct coupling between accretion flow vorticity, disk plasma diffusivity and the large scale ordered magnetic field which may have directly observable implications (Contopoulos et al. 2009).

The magnetic field loops generated by the action of the Cosmic Battery around the inner edge of the accretion disk (where radiation pressure and aberration effects are maximal) are anchored on different radii of the inner accretion disk, thus they become twisted in the azimuthal direction by the differential rotation of the flow. As their twisting relaxes in the vertical direction, the loops open up and separate into an inner component and an outer

component (the return field) that threads the disk further away from the axis. The poloidal fields of the two components are in opposite directions, the inner one is parallel and the outer one is antiparallel to the angular velocity vector. On top of that, an overall helical magnetic field is produced when the footpoints of the initially poloidal magnetic field loops are dragged by the rotating disk plasma, with the inner toroidal magnetic field pointing in the direction opposite to that of the disk rotation in the northern hemisphere of the disk, and along the direction of the disk rotation in the southern hemisphere. According to the Cosmic Battery, reversing the observer's hemisphere, or equivalently, the direction of disk rotation, reverses the polarity of the axial field but leaves the direction of the toroidal field unchanged in the observer's sky. This can be tested in radio VLBI jets, where the direction of the toroidal field can be directly inferred from measurements of Faraday rotation gradients transverse to the jet axis (Blandford 1993, Reichstein & Gabuzda 2012, Murphy & Gabuzda 2013). Observations of the toroidal fields revealed from such measurements in pc-scale jets from active galactic nuclei show that, in most cases, the axial electric current in the VLBI core jet flows toward the center (Contopoulos et al. 2009). The probability that this asymmetry came about by chance was calculated to be less than 1%. This observational result supports the hypothesis that the universe is seeded by cosmic magnetic fields that are generated in active galactic nuclei via the mechanism of the Cosmic Battery, and are subsequently injected in intergalactic space by the jet outflows.

In the original Cosmic Battery paper (CK) we studied the Poynting-Robertson effect of a central isotropic radiation field on the evolution of the magnetic field in a thin accretion flow. We followed the evolution of the magnetic

\* icontop@academyofathens.gr

field by solving the induction equation in 1D under the assumption that the generated magnetic field is purely vertical. We extended this analysis in axisymmetric configurations (2D; Contopoulos et al. 2006, Christodoulou et al. 2008) under the assumption that the accretion disk is connected to a steady-state force-free magnetosphere above and below it. Our work faced some criticisms. The main argument against the Cosmic Battery consists of the misconception that the poloidal magnetic field loops advected to the center saturate the magnetic field to values well below equipartition (Bisnovatyi-Kogan et al. 2002). This criticism does not take into account the fact that because the loops are stretched by the differential rotation, they open up vertically, and only the inner part of the loop is advected inward. In most cases of astrophysical significance, the outer part of the loop diffuses outward because astrophysical accretion disks are turbulent and viscous, thus also diffusive, and the field growth does not saturate.

We decided to extend our previous axisymmetric simulations to realistic astrophysical scenarios. We consider general hot accretion flows around a spinning black hole. The main new element of our present simulations is that we now follow the time-dependent evolution of the force-free magnetospheric field. As we will see, the magnetospheric field is twisted by the differential rotation in the disk and the central spinning black hole. The inner part is advected toward the black hole horizon, and the outer part diffuses through the outer accretion disk. We obtained several animations (movies) of the field evolution which the interested reader may find in the web (e.g. <http://youtu.be/keF0V8xwons>). Our present analysis is Newtonian (i.e. non-general relativistic), but we expect it to be also valid qualitatively when generalized in general relativity.

In § 2 we present a brief overview of various disk models, and outline the main physical processes that we consider in our integration of the induction equation. In § 3 we discuss how we couple the disk with a force-free magnetosphere above and below it. In § 4 we discuss the fundamental importance of the magnetic Prandtl number with two characteristic examples, one that exhibits continuous magnetic field growth, and one that exhibits saturation of the mechanism. Finally, in § 5 we discuss various astrophysical examples of ADAF disks and reach our conclusions.

## 2. ADAF DISKS AND THE INDUCTION EQUATION

Black hole accretion is a physical process that provides the primary source which powers active galactic nuclei (hereafter AGN), black hole X-ray binaries (hereafter XRB) and possibly also gamma-ray bursts (hereafter GRB). Black hole accretion flows are divided into two categories, cold and hot. Cold accretion flows are described by the standard thin disk model (Shakura & Sunyaev 1973, Novikov & Thorne 1973, Lynden-Bell & Pringle 1974). In this case the disk is geometrically thin but also optically thick and quite cold. The thin disk model is applicable when the mass accretion rate is somewhat below the Eddington rate. In this paper we study the cosmic battery in the general case of a hot accretion flow around a rotating black hole.

The first model for hot accretion was obtained by Shapiro et al. (1976). In this case the plasma is more

tenuous and hotter than the plasma in a thin disk, and is also optically thin. The main characteristic of this model is the introduction of a two-temperature accreting plasma where the ions have higher temperature than the electrons. This model succeeded for the first time in explaining the hard X-ray emission seen in black hole sources. Unfortunately, it is thermally unstable, and therefore it cannot be a good representation for astrophysical accretion disks. Ichimaru (1977) was the first who studied the important role of advection in hot accretion flows. He pointed out that, in certain regimes, the viscously dissipated accretion energy can go preferentially into heating the accretion flow than into radiation (Ichimaru 1977, Rees et al. 1982, Yuan & Narayan 2014). This is the central element of advection dominated accretion flows (hereafter ADAF). The discovery of ADAF solutions (Narayan & Yi 1994, Narayan & Yi 1995a, Narayan & Yi 1995b, Abramowicz et al. 1995, Chen et al. 1995, Yuan & Narayan 2014) gave rise to the application of ADAF models in various black hole systems. These systems include the supermassive black hole in the Galactic center, Sagittarius A, low-luminosity AGNs and black hole X-ray binaries (e.g. Narayan et al. 1998, Abramowicz & Fragile 2013, Narayan & McClintock 2008, Ho 2008, Quataert 2001, Lasota 1999).

ADAF models are characterized by the following six equations for the radial velocity  $v_r$ , the azimuthal velocity  $v_\phi$ , and the isothermal sound speed  $c_s$  (Narayan & Yi 1994),

$$\begin{aligned} v_r &= -\frac{3a}{5+2\epsilon/f} v_K \\ v_\phi &= \frac{2\epsilon/f}{5+2\epsilon/f} v_K \\ c_s &= \left( \frac{2}{5+2\epsilon/f} \right)^{1/2} v_K, \end{aligned} \quad (1)$$

where,  $v_K \equiv (GM/r)^{1/2}$  is the Keplerian velocity,  $M$  is the mass of the central compact object/black hole, and  $c_s$  is the speed of sound.  $\epsilon = \frac{(\frac{5}{2}-\gamma)}{(\gamma-1)}$  where  $\gamma$  is the ratio of specific heats.  $\gamma = \frac{4}{3}$  in a relativistic plasma. The advection parameter  $0 < f \leq 1$  measures the fraction of the viscously generated heat that is advected with the flow. When  $f \rightarrow 1$ , most of the generated heat is advected with the flow, whereas when  $f \rightarrow 0$  the accretion flow radiates away all of its generated heat. In that case we end up with a standard thin Shakura-Sunyaev disk (Shakura & Sunyaev 1973) with accretion constant  $a \approx 0.1$  (this value corresponds to accretion disks around black holes; Komissarov 2006). We will henceforth work in spherical coordinates  $(r, \theta, \phi)$ . Notice that the expression for the sound speed is needed in order to determine the scale height of the disk  $h \equiv rc_s/v_K$ , or equivalently the polar angle of the surface of the disk

$$\theta_{\text{disk}} \equiv \cos^{-1} \left( \frac{h}{r} \right) = \cos^{-1} \left( \frac{c_s}{v_K} \right). \quad (2)$$

Eqs. (1) are non-relativistic. On the other hand, the Cosmic Battery is most effective around the inner edge of the accretion disk around an astrophysical black hole which is believed to coincide with the radius of the in-

nermost stable circular orbit (hereafter ISCO). We do not plan to perform a full general relativistic numerical simulation in that region. Instead, we extend our Newtonian formulation down to the black hole horizon. We believe that, the exact details of the accretion flow in that region are not particularly important. As we will see below, what is most important is the fact that *inside the ISCO, the flow transitions from being mostly Keplerian, thus also turbulent, viscous, and diffusive, to being mostly freely falling, thus also laminar, non-viscous, and non-diffusive.*

Our aim in this paper is to investigate the action of the Cosmic Battery in realistic astrophysical accretion disks. We will thus assume the above velocity profile inside the disk (eqs. 1) and integrate the induction equation (eq. 3 below) in order to follow the evolution of the disk magnetic field in the presence of the Cosmic Battery radiation source. In other words, we will assume that the field is passive and does not affect the velocity field in the disk.

The induction equation in the disk ( $\theta_{\text{disk}} \leq \theta \leq 90^\circ$ ) can be written as

$$\frac{\partial \mathbf{B}_{\text{disk}}}{\partial t} = -c \nabla \times \left( E_{\text{CB}} \hat{\phi} - \frac{v}{c} \times \mathbf{B}_{\text{disk}} + \eta \nabla \times \mathbf{B}_{\text{disk}} \right) \quad (3)$$

where  $\mathbf{B}_{\text{disk}}$  is the magnetic field, and  $\eta$  is the magnetic diffusivity in the disk. The Cosmic Battery electromotive source term  $E_{\text{CB}}$  is equal to the aberrated radiation force on the electrons in the azimuthal direction  $F_{\text{rad}}|_\phi$  divided by the proton charge  $e$ . In our original paper, we considered a simplified central radiation field with luminosity  $L$ , in which

$$E_{\text{CB}} = \frac{F_{\text{rad}}|_\phi}{e} = -\frac{L\sigma_T}{4\pi c e r^2} \frac{v_\phi}{c} \quad (4)$$

where,  $\sigma_T$  is the electron Thompson cross section. The correct expression for the aberrated radiation force requires a complex general relativistic calculation of the radiation field as felt by the moving electron, taking into consideration the plasma optical depth and the fact that the source of radiation is the accretion disk itself. This calculation has been performed for the first time by Koutsantoniu & Contopoulos (2014) for an optically thick flow with a thermally emitting surface. The case of an optically thin disk is much more complex and is currently under investigation. In order to proceed, we will assume a slightly more general phenomenological expression

$$E_{\text{CB}} = -\frac{L\sigma_T}{4\pi c e r^2} \frac{v_\phi}{c} \times \begin{cases} 1 \text{ or } e^{-\frac{(r-r_{\text{ISCO}})^2}{2r_{\text{ISCO}}^2}} & \text{if } r \geq r_{\text{ISCO}} \\ e^{-\frac{(r-r_{\text{ISCO}})^2}{2(0.2r_{\text{ISCO}})^2}} & \text{if } r < r_{\text{ISCO}} \end{cases} \quad (5)$$

which incorporates the main features of a realistic radiation force: the buildup of the radiation field as we approach the ISCO, the Poynting-Robertson (radiation aberration) effect, and the  $1/r^2$  drop-off with distance of the radiation pressure in an optically thin medium. We also have the option to account for some long optical depth (on the order of  $r_{\text{ISCO}}$ ) in the disk (second expression in top line of eq. 5 above). As we said above, a more detailed general relativistic calculation of the radiation force that takes into account the physical optical depth of the accretion flow is under way (Koutsantoniu

& Contopoulos in preparation).

The magnetic diffusivity  $\eta$  can be expressed as

$$\eta = \begin{cases} \frac{arc_s^2}{v_K \mathcal{P}_m} & \text{if } r \geq r_{\text{ISCO}} \\ 0 & \text{if } r < r_{\text{ISCO}} \end{cases} \quad (6)$$

(see for example Lovelace et al. 2009). The magnetic diffusivity is therefore a function of the magnetic Prandtl number  $\mathcal{P}_m$  which itself is in general a function of distance in the accretion flow. In the present work we will assume that  $\mathcal{P}_m$  is roughly a constant within the spatial extent of our numerical simulations, but very quickly becomes infinite (i.e.  $\eta$  drops very quickly to zero) inside  $r_{\text{ISCO}}$  as the flow very quickly changes character from quasi-Keplerian to almost free fall on the black hole horizon. This transition is related to the fact that as the flow rotation decreases, the shear decreases, and the flow becomes laminar inside the ISCO because matter is almost in free fall there. The laminar flow implies that the turbulence responsible for both the flow viscosity and the magnetic diffusivity ceases.

### 2.1. Numerical setup

We solve our equations in a numerical grid with uniform latitudinal spacing  $\delta\theta$ , linearly increasing radial spacing  $\delta r = 3r\delta\theta$ , and a finite radial extent  $r_{\text{in}} \leq r \leq r_{\text{out}}$ , where  $r_{\text{in}} = r_{\text{ISCO}}/3$ , and  $\theta_{\text{min}} \leq \theta \leq 90^\circ$ . Although our formalism is Newtonian, the inner radial boundary  $r_{\text{in}}$  of our grid is taken to represent the black hole horizon. An inner polar cutoff of a few degrees  $\theta_{\text{min}} \sim 5^\circ$  is implemented in order to avoid coordinate system singularities around the axis. Our standard  $r \times \theta$  grid resolution is  $87 \times 90$  respectively, and our numerical grid extends radially out to  $r_{\text{out}} = 25r_{\text{ISCO}}$ . We have also run selected simulations with double grid resolution, namely  $174 \times 180$ , and found agreement within less than 5%. We have thus concluded that our present numerical results have converged. We have also run simulations on a uniform  $(\delta r, \delta\theta)$  grid and obtained essentially the same results.

The magnetic field is generated by the Cosmic Battery and is not brought in from large distances, therefore, the time integration of eq. (3) begins with

$$\mathbf{B}_{\text{disk}}(t=0) = 0. \quad (7)$$

Also, we set  $B_r = B_\phi = 0$  along the equator  $\theta = 90^\circ$ , and implement free inner and outer boundaries at  $r_{\text{in}}$  and  $r_{\text{out}}$  respectively. What is most important is that the magnetic field along the surface of the disk is matched to the magnetospheric field, namely

$$\mathbf{B}_{\text{disk}}(\theta_{\text{disk}}) = \mathbf{B}_{\text{MS}}(\theta_{\text{disk}}). \quad (8)$$

The magnetospheric field  $\mathbf{B}_{\text{MS}}(r, \theta)$  for  $\theta \leq \theta_{\text{disk}}$  is obtained in an independent calculation that we are now going to discuss.

### 3. THE FORCE-FREE MAGNETOSPHERE

Whenever the magnetic field generated by the Cosmic Battery in the disk reaches the surface it will extend into the disk atmosphere, the so-called magnetosphere. In order to follow the evolution of the magnetic field in the accretion flow, we must also numerically evolve the

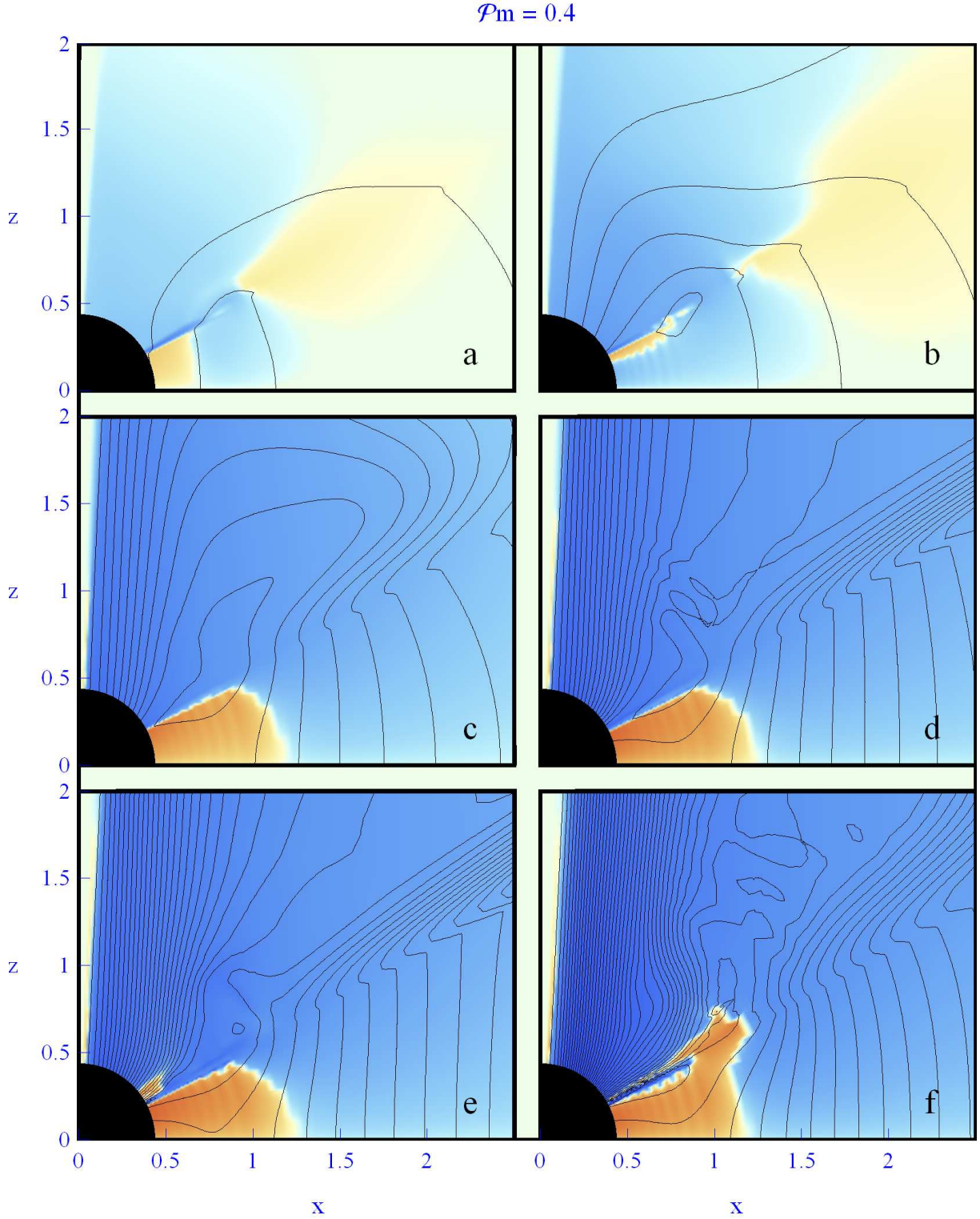


**Figure 1.** Poloidal magnetic field lines at times  $t_{\text{acc}}$  (a),  $3t_{\text{acc}}$  (b),  $8.6t_{\text{acc}}$  (c),  $15.7t_{\text{acc}}$  (d),  $23.7t_{\text{acc}}$  (e), and  $38.4t_{\text{acc}}$  (f), in the standard case of a diffusive accretion disk with Prandtl number  $\mathcal{P}_m = 0.4$ . Length scales in unit of  $r_{\text{ISCO}}$ . Colors represent the value and sign of  $B_\phi$  in arbitrary units (blue: negative, orange: positive). The surface of the disk lies at  $\theta = 60^\circ$ . Poloidal field loops are continuously generated around  $r_{\text{ISCO}}$ . The inner footpoints of the field lines are advected together with infalling matter to the central object, and magnetic flux of one polarity is accumulated on the central object at a steady rate. The disk is threaded by the return field polarity. The outer footpoints are diffusing outwards inside the accretion disk, and because of the differential rotation of their footpoints, the loops open up. A steady configuration is established where poloidal loops are continuously generated around the inner edge of the disk and open up to infinity.

field in the magnetosphere just above the surface of the disk. It is natural to assume that, near the surface of the disk, the magnetosphere attains a force-free configuration, in analogy to the solar corona and the pulsar magnetosphere. The equations that describe the field evolution are those of force-free electrodynamics (FFE; Gruzinov 1999, Blandford 2002), namely Maxwell's equations in the presence of electric charges and currents,

$$\begin{aligned}\frac{\partial \mathbf{B}_{\text{MS}}}{\partial t} &= -c \nabla \times \mathbf{E}_{\text{MS}} \\ \frac{\partial \mathbf{E}_{\text{MS}}}{\partial t} &= c \nabla \times \mathbf{B}_{\text{MS}} - 4\pi \mathbf{J} \\ \nabla \cdot \mathbf{B}_{\text{MS}} &= 0 \\ \nabla \cdot \mathbf{E}_{\text{MS}} &= 4\pi \rho_e ,\end{aligned}\quad (9)$$

supplemented by the force-free and ideal MHD conditions

$$\rho_e \mathbf{E}_{\text{MS}} + \mathbf{J} \times \mathbf{B}_{\text{MS}} = 0 \quad (10)$$

$$\mathbf{E}_{\text{MS}} \cdot \mathbf{B}_{\text{MS}} = 0 . \quad (11)$$

Here,  $\rho_e$ ,  $\mathbf{J}$  are the magnetospheric electric charge and current densities respectively. The above formulation is obviously non-general relativistic, yet we believe that the simulations performed in this study can give an overall impression about how the Cosmic Battery mechanism works. Notice that recent general relativistic simulations of force-free disk magnetospheres (Parfrey et al. 2015) show a magnetic field evolution similar to the one we obtain here (magnetic field loops becoming twisted and opening up due to the differential rotation of the flow in the disk, current sheet and plasmoid formation, etc.). We plan to extend our numerical calculations in general relativity in a forthcoming paper.

### 3.1. Numerical setup

The numerical code we employ is the 3D code first developed in Kalapotharakos & Contopoulos (2009), rewritten in spherical coordinates  $(r, \theta, \phi)$  by Contopoulos (2013). We have lowered the dimensions to 2D by assuming axisymmetry. As in the disk interior, we implement an inner free boundary at  $r = r_{\text{in}}$  in this region too. In practice, we allow for any magnetic flux that is generated inside the disk and reaches the inner magnetospheric boundary (which represents the black hole horizon), to be freely distributed along that boundary. Beyond a certain distance  $r_{\text{PML}} < r_{\text{out}}$ , we assume an absorbing non-reflecting outer boundary in the form of a special implementation of an axisymmetric Perfectly Matched Layer (PML; discussed in detail in Kalapotharakos & Contopoulos 2009), namely

$$\begin{aligned}\frac{\partial \mathbf{B}_{\text{MS}}}{\partial t} &= -c \nabla \times \mathbf{E}_{\text{MS}} - \sigma(r) \mathbf{B}_{\text{MS}} \\ \frac{\partial \mathbf{E}_{\text{MS}}}{\partial t} &= c \nabla \times \mathbf{B}_{\text{MS}} - \sigma(r) \mathbf{E}_{\text{MS}} ,\end{aligned}\quad (12)$$

where

$$\sigma(r) = \sigma_o \frac{c}{r_{\text{ISCO}}} \left( \frac{r - r_{\text{PML}}}{r_{\text{out}} - r_{\text{PML}}} \right)^3 . \quad (13)$$

We have taken  $\sigma_o = 100$ , and  $r_{\text{PML}} = 17r_{\text{ISCO}}$ . These parameters, as well as the exponent in eq. (13) have been

chosen empirically. Notice the similarity with the equivalent expression in Cerutti et al. (2014). We have run several simulations at various radial resolutions and various values of the outer boundary  $r_{\text{out}}$  and the results are similar (the simulations have converged). For most of the results we obtain in the present paper, the outer boundary was placed at  $25r_{\text{ISCO}}$ .

As we said in the previous section, the evolution of the magnetic fields in the two domains (the disk and the magnetosphere) are related. It is important to notice here that there is an important complication that enters in the matching between the two domains, and this has to do with the abrupt transition between the dense turbulent accreting flow and the almost empty ionized (probably also evaporating and outflowing) magnetosphere. This is very similar to the well known transition region in the sun where, within a very thin layer of about one hundred kilometers, the temperature rises by almost two orders of magnitude to about one million degrees, and the matter density drops by about one order of magnitude. The solar transition region is the subject of ongoing intense theoretical and numerical investigations. The astrophysical disk transition region is at least equally complicated since it is not only the base of the disk corona, but also the origin of purported disk winds and outflows (e.g. Li 1995, Ferreira & Pelletier 1995). is not the aim of the present study to solve in detail for the structure of the flow and magnetic field in this region. In practice, we define a transition region of two  $\theta$ -grid zones above  $\theta_{\text{disk}}$ . In that region we set

$$\mathbf{B}_{\text{MS}} = \mathbf{B}_{\text{disk}} . \quad (14)$$

This matching allows for magnetic field loops that reach the disk surface zones to escape to the magnetosphere. We also set the field lines in that region in rotation by introducing a magnetospheric poloidal electric field

$$\mathbf{E}_{\text{MS}}(\theta_{\text{disk}}) = -\frac{v_\phi}{c} \hat{\phi} \times \mathbf{B}_{\text{disk}}(\theta_{\text{disk}}) . \quad (15)$$

Finally, we slightly modify the induction equation that we solve for the disk material in that region by introducing an extra phenomenological term that mimics various complex physical effects taking place in the surface layers of astrophysical accretion disks such as surface convection, buoyancy of magnetic field loops, and the fact that the surface layers are highly ionized (thus also fully conducting) due to cosmic ray irradiation, namely

$$\frac{\partial \mathbf{B}_{\text{trans}}}{\partial t} = -c \nabla \times \left( E_{\text{CB}} \hat{\phi} + \frac{1}{200} \hat{\theta} \times \mathbf{B}_{\text{trans}} \right) , \quad (16)$$

where,  $\mathbf{B}_{\text{trans}}$  is the disk magnetic field in the. The introduction of this transition layer effectively shields the disk interior: a) it prevents any generated magnetospheric field from ‘entering’ the disk from above (especially in the case of turbulent high  $\eta$  flow conditions), and b) it ‘pushes outward’ (in the  $\theta$  direction) at a very small fraction of the speed of light any magnetic field loop that enters it from below. We implemented different fractions (1/200, 1/20, etc.) and the results were qualitatively similar. transition region. As we said above, we are not claiming that we study in detail the disk-magnetosphere transition region. This is the reason we opted for a minimal two  $\theta$ -zone layer that only serves the purpose of

shielding the disk interior from the disk magnetosphere. Notice that Parfrey et al. (2015) ignored the important physical significance of a transition layer by directly coupling their magnetosphere to a prescribed distribution of the magnetic field on the surface of the accretion disk, *without* solving for the magnetic field distribution in the disk interior.

The inner boundary (which represents the black hole horizon) also introduces a rigid body rotation expressed through

$$\mathbf{E}_{\text{MS}}(r_{\text{in}}, \theta) = -\frac{v_{\phi}(r_{\text{in}}, \theta_{\text{disk}}) \sin(\theta)}{c \sin(\theta_{\text{disk}})} \hat{\phi} \times \mathbf{B}_{\text{MS}}(r_{\text{in}}, \theta) \quad (17)$$

for  $\theta \leq \theta_{\text{disk}}$ . The latter turns out not to be important in the determination of the overall magnetospheric field topology, and plays a role only if we are interested in the extraction of energy from the black hole rotation (Blandford & Znajek 1977). As in the disk interior, the time integration of eqs. (9-12) begins with

$$\mathbf{B}_{\text{MS}}(t = 0) = 0 \quad (18)$$

everywhere in the magnetosphere.

#### 4. THE COSMIC BATTERY IN ACTION

The goal of this paper is to convince the reader that the Cosmic Battery plays a fundamental role in the generation of the large scale magnetic fields that thread astrophysical accretion disks and are believed to be responsible for such diverse astrophysical phenomena as jets, AGNs, XRBs, and possibly also GRBs. We performed numerical integrations that couple the FFE equations in the magnetosphere above and below the disk (eqs. 9-11) with the induction equation that includes the Cosmic Battery electromotive force and the flow magnetic diffusivity in the disk (eq. 3). As we said, the coupling is performed in a thin surface transition region through eqs. (14-16). Our goal is to find out how much magnetic flux can be accumulated around the central compact object. In particular, we are going to show under what conditions the accumulated magnetic flux grows steadily to equipartition, and under what conditions it saturates to a very low value. We want to make clear that these are not MHD flow simulations since the accretion flow is independently specified by the ADAF equations (eqs. 1).

In this section, we are going to highlight the fundamental role of the accretion disk magnetic diffusivity in activating (or under different conditions saturating) the Cosmic Battery. This point, already discussed in the original CK presentation, has been missed by Bisnovatyi-Kogan et al. (2002) in their criticism of the Cosmic Battery. We will thus now focus on two particular simulations, one with moderate and one with low magnetic diffusivity. The first simulation corresponds to a magnetic Prandtl number  $\mathcal{P}_m = 0.4$ . We will call this case the ‘*standard*’ case. In the second simulation we set  $\mathcal{P}_m = 100$ . We will call this case the ‘*very low  $\eta$* ’ case. Notice that, in order to minimize the number of free parameters in the problem, we fix the accretion constant  $a = 0.1$ , and the advection parameter  $f = 1$  (the latter value corresponds to a strongly advection-dominated flow). We will now compare the evolution of our two characteristic simulations.

In the beginning, the Cosmic Battery term (eq. 5) generates poloidal magnetic loops around  $r_{\text{ISCO}}$  in both

cases. The inner footpoints of the field lines are advected by disk matter that falls into the central object. Furthermore, as each loop enters the magnetosphere it starts to inflate due to the differential rotation between its inner and outer footpoints on the surface of the disk. This can be seen in Figs. 1a and 2a which are very similar. As the mechanism continues to operate, more and more field lines are brought to the central object. The similarities end beyond about one accretion time defined as the time needed to traverse a distance equal to  $r_{\text{ISCO}}$  at the ISCO accretion speed, namely

$$\begin{aligned} t_{\text{acc}} &\equiv \frac{r_{\text{ISCO}}}{v_r(r_{\text{ISCO}})} \\ &= \left( \frac{5 + 2\epsilon/f}{3a} \right) \frac{r_{\text{ISCO}}}{v_K(r_{\text{ISCO}})} \\ &\approx 1.7 \times 10^{-2} \left( \frac{M}{10M_{\odot}} \right) \text{ sec} . \end{aligned} \quad (19)$$

What differentiates the two cases is the behavior of the outer footpoints beyond that time.

##### 4.1. The standard case

In the standard case, the outer footpoint of a poloidal field line generated by the Cosmic Battery begins to diffuse outward inside the accretion disk. Because of the difference in the rotation between the two footpoints, the field lines wind up around the central object. They inflate in the magnetosphere above the accretion disk and sustain a connection between the central object and the disk (Fig. 1b). New loops are continuously generated around the position of the ISCO (Fig. 1b-f). As the outer footpoints are continuously moving outward, the loops expand more and more. Their inner and outer parts never disconnect, and the sign of the magnetospheric  $B_{\phi}$  component remains unchanged (negative). Notice that although  $B_{\phi}$  develops highly variable structure on small scales (as can be seen in Figs. 1e & f), it does not affect the large scale field structure, and the numerical integration is stable. The return polarity diffuses outward and the field in the disk remains at very low (sub-equipartition) values. Such low magnetic field cannot be responsible for a disk MHD wind (e.g. Li 1995, Ferreira & Pelletier 1995). This is an interesting point that may be investigated more in the future.

If the central object is rotating, then the field lines of one polarity that have already reached it can extract its rotational energy (Blandford & Znajek 1977, Nathanail & Contopoulos 2014). In this paper, we are interested in showing the growth of the magnetic field, and therefore, we are not going to discuss this effect any further. It is interesting to notice that, for the particular ADAF parameters of our present simulation, the inner magnetospheric boundary is set in uniform rotation with  $\Omega(r_{\text{in}}) = \Omega_{\text{disk}}(r_{\text{in}}, \theta_{\text{disk}}) = 0.6c/r_{\text{ISCO}}$ . This corresponds to a magnetospheric light cylinder at cylindrical radius

$$R_{\text{LC}} \equiv \frac{c}{\Omega(r_{\text{in}})} = 1.67 r_{\text{ISCO}} . \quad (20)$$

As shown in Fig. 3, the magnetic flux brought to the central object grows at a steady rate which has no reason to cease before the field reaches equipartition with the accretion flow (defined as the limit where the accu-



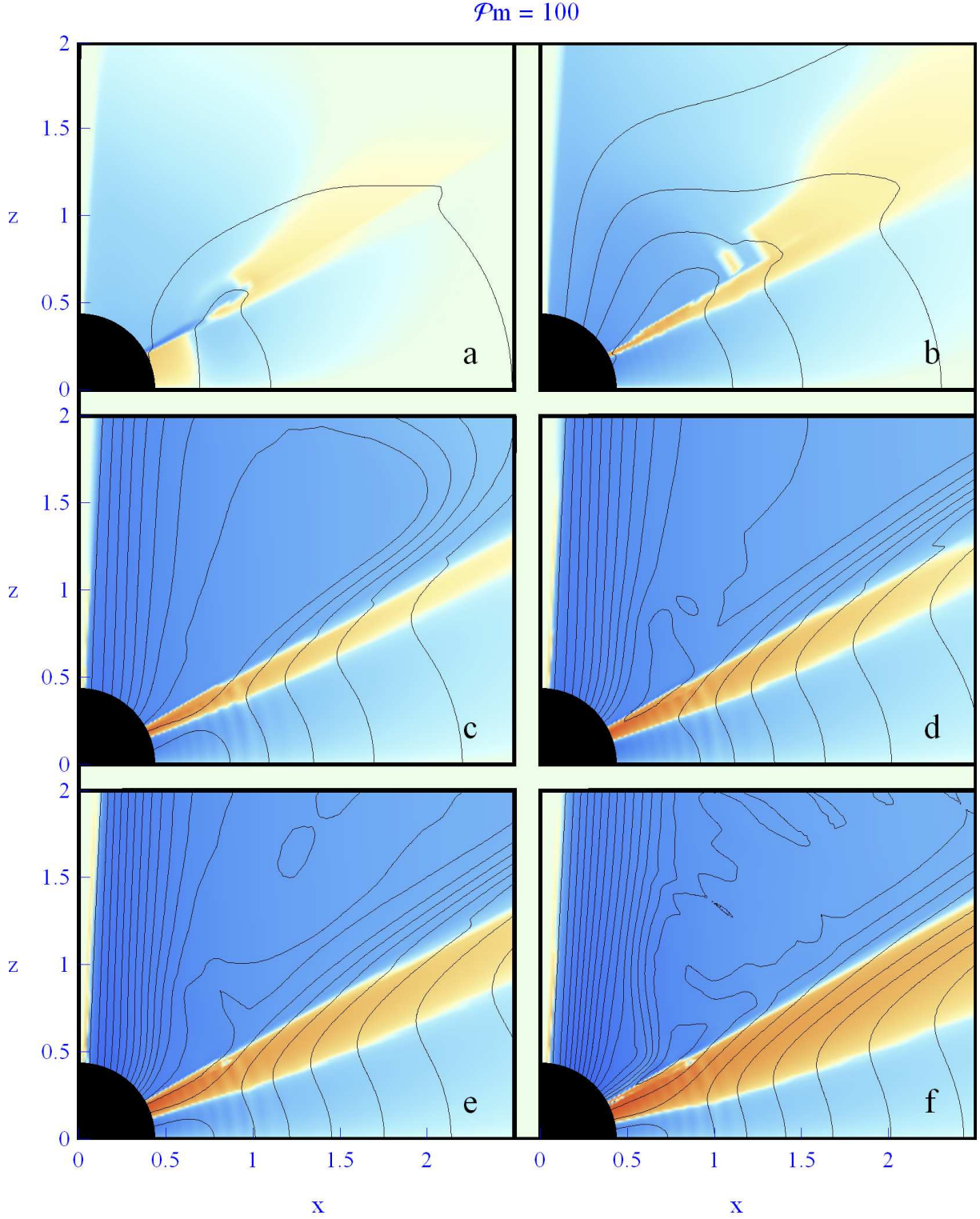


**Figure 2.** Same as Fig. 1 for the very low  $\eta$  case of a non-diffusive optically thin accretion disk with magnetic Prandtl number  $\mathcal{P}_m = 100$ . The inner footpoints of the field lines are advected together with infalling matter onto the central object. In the outer disk region there is a balance between inward advection (that wants to bring the outer footpoints to the central object), outward diffusion, and continuous field generation due to the action of the Cosmic Battery. The rate of growth of the accumulated magnetic field keeps decreasing and eventually saturate.

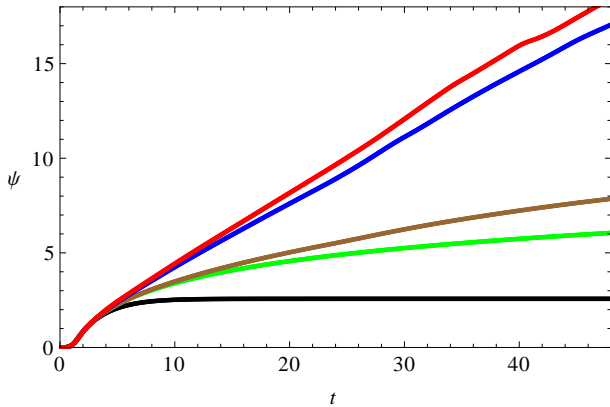


**Figure 3.** Evolution of the magnetic flux  $\Psi$  accumulated on the central object (in units of  $\Psi_{\text{acc}}$ ) for various values of the magnetic Prandtl number (from top to bottom:  $\mathcal{P}_m = 0.2, 0.4, 1, 10, 100$ , and 100 with finite optical depth in the disk). Time in units of  $t_{\text{acc}}$

culated magnetic field pressure  $B^2/4\pi$  becomes comparable to the ram pressure  $\rho v_r v_\phi$  of the flow). In Fig. 3, we have normalized  $\Psi$  to a characteristic value  $\Psi_{\text{acc}}$  that corresponds to the amount of flux accumulated interior to  $r_{\text{ISCO}}$  generated by the Cosmic Battery electromotive force term in one accretion time, namely

$$\begin{aligned} \Psi_{\text{acc}} &\equiv \frac{\pi r_{\text{ISCO}}^2 E_{\text{CB}}(r_{\text{ISCO}}) c}{v_r(r_{\text{ISCO}})} \\ &= \left( \frac{v_\phi}{v_r} \right) \frac{L \sigma_T}{4 c e} \approx \frac{\epsilon}{6 f a} \frac{L \sigma_T}{c e} \\ &\approx 10^{14} \text{ G cm}^2 \left( \frac{L}{L_{\text{Edd}}} \right) \left( \frac{M}{10 M_\odot} \right) \\ &\approx 0.4 \text{ G } \pi r_{\text{ISCO}}^2 \left( \frac{L}{L_{\text{Edd}}} \right) \left( \frac{M}{10 M_\odot} \right)^{-1}. \quad (21) \end{aligned}$$

What is important to notice is that the magnetic field that threads the disk interior remains always at a very low value since, inside the ISCO it is continuously advected toward the central boundary (the black hole horizon), whereas outside it is continuously diffusing outward through the accretion disk. As long as the field remains at such small values, the MRI, the physical mechanism believed to be responsible for the disk turbulence (Balbus & Hawley 1992), does not saturate.

#### 4.2. The very low $\eta$ case

The field evolution in the very low  $\eta$  case is very different. Beyond the accretion time  $t_{\text{acc}}$  needed for matter to reach the central object, the mechanism begins to saturate. As we pointed out above (and as can be seen in Fig. 2a), at times up to a few times  $t_{\text{acc}}$  the evolution is the same as in the standard case, namely the inner field footpoints are carried by matter falling to the central object and the outer footpoints are rotating with the disk. However, the accretion disk is no longer diffusive and the outer footpoints do not diffuse easily outward inside the disk. In fact, the accretion flow wants to bring also the outer footpoints to the central object. The whole loop would be swallowed by the central object, but this is not the case since new magnetic field loops are continuously generated by the Cosmic Battery in the optically thin part of the disk. Due to this, the mechanism instead saturates. We see the deviation from the standard case

already at times  $t \sim 10 t_{\text{acc}}$  when the inner and outer parts of the poloidal magnetic field loops begin to disconnect (Fig. 2b,c). Beyond that time, the field lines of the return polarity which are anchored at larger distances on the disk are now wound by the disk rotation at their footpoints, and not by the differential winding between the inner and outer footpoints of the loop (which, as we said, are now disconnected). When this happens, the  $B_\phi$  component of the return (outer) field line changes sign (becomes positive), as can be seen by the change of color near the surface of the disk. A dynamic magnetospheric current sheet forms between the two regions of opposite poloidal field polarity which in our very-low  $\eta$  case lies a few degrees above the surface of the disk (Figs. 2d-f). The ongoing (numerical) reconnection forms plasmoids that outflow fast along the current sheet. Plasmoid formation and reconnection in the current sheet may be responsible for particle acceleration and dissipation of energy. Magnetic flux is continuously advected on the central object, but at a continuously reduced rate (see Fig. 3).

We have also run simulations in which we implement a long but finite optical depth in the disk according to the second term in the first line of eq. 5, for the same value of the disk diffusivity (low  $\eta$ ). This effectively kills the Cosmic Battery beyond a radial distance of a few  $r_{\text{ISCO}}$ . In that case, the field saturation is much clearer as can be seen in Figs. 3 & 4.

Notice that, in the very low  $\eta$  case, the saturation value of the magnetic flux that was brought to the central object is very low, thus, the observed current sheet activity observed in this case is probably astrophysically insignificant. The big difference from the standard case is that in the latter, the magnetic flux continues to grow at a steady rate, presumably up to equipartition.

## 5. DISCUSSION AND CONCLUSIONS

In the previous section we argued that the main factor that allows for the steady growth of the accumulated magnetic flux is the value of the magnetic Prandtl number  $\mathcal{P}_m$  in the disk. We run several simulations for different values of the magnetic Prandtl number in the accretion flow (Fig. 3). In these simulations, other physical parameters are kept constant. It is interesting to see that in all our runs the magnetic flux advected to the central object within a few accretion times  $t_{\text{acc}}$  remains almost the same (on the order of  $\Psi_{\text{acc}}$ ). Within that short amount of time, the mechanism does not feel the diffusivity properties of the disk. As time goes by, only diffusive disks allow the magnetic flux to grow. As can be seen in Fig. 3, the rate of growth is closely coupled with the magnetic diffusivity of the disk. When the Prandtl number is low (high diffusivity), the rate of growth is bigger. For the lowest values that we have tried ( $\mathcal{P}_m = 0.2, 0.4, 1$ ), the growth of the magnetic flux is linear with similar slope after about  $t_{\text{acc}}$  from the beginning of the run. As the Prandtl number increases beyond unity (which corresponds to lower and lower diffusivity), the rate of growth of the magnetic flux continuously decreases with time, approaching zero asymptotically (no growth, i.e. saturation). There seems to be a critical value of the magnetic Prandtl number for this transition in the range  $1 < \mathcal{P}_{m \text{ crit}} < 10$ . For Prandtl numbers higher than 100 the situation is identical to the very low



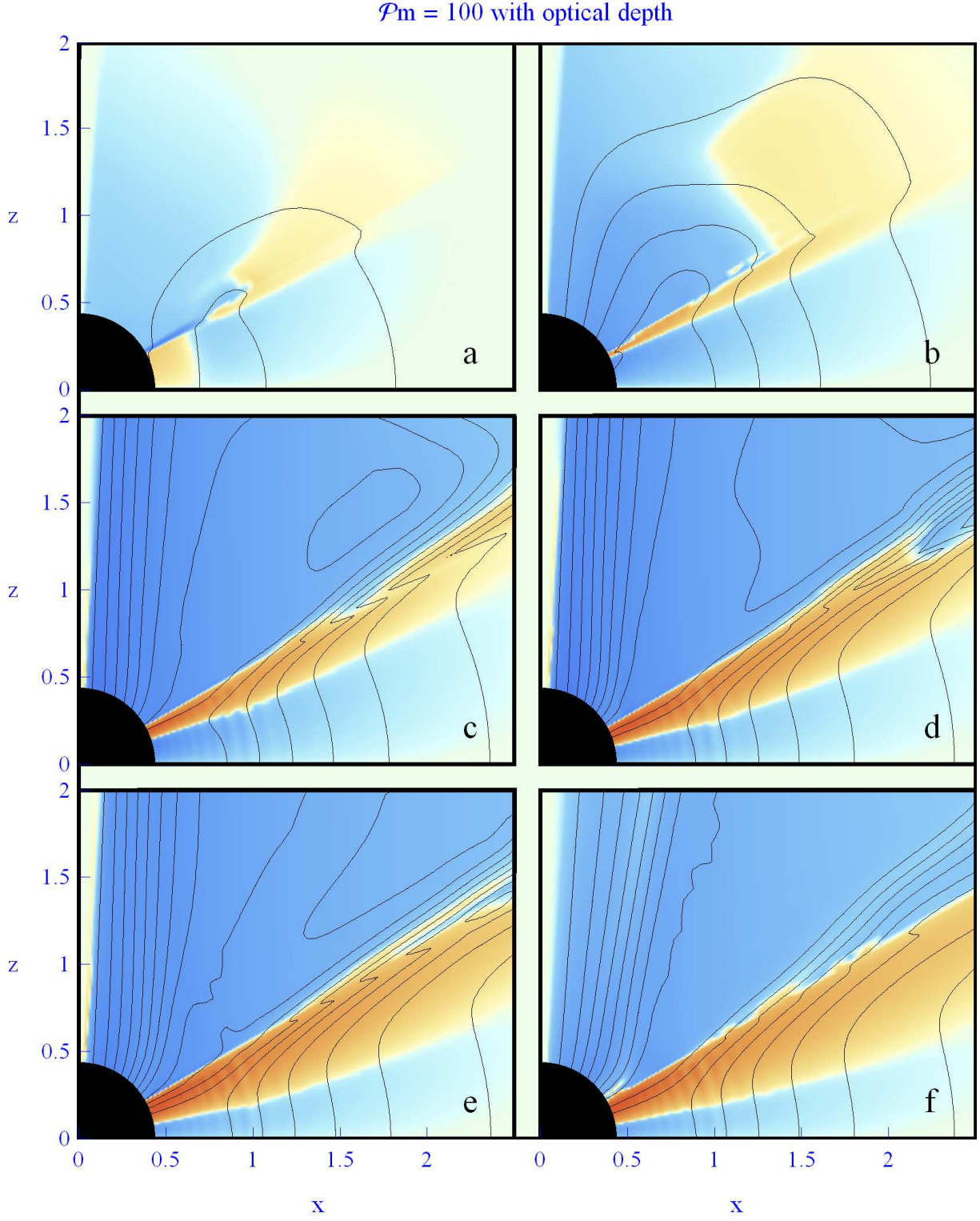


**Figure 4.** Same as Fig. 2 but now an optical depth of order  $r_{\text{ISCO}}$  is included in the disk and the Cosmic Battery dies out beyond a few times  $r_{\text{ISCO}}$ . Saturation is reached very quickly and beyond time  $t \approx 5t_{\text{acc}}$  no more magnetic flux is brought to the central object.

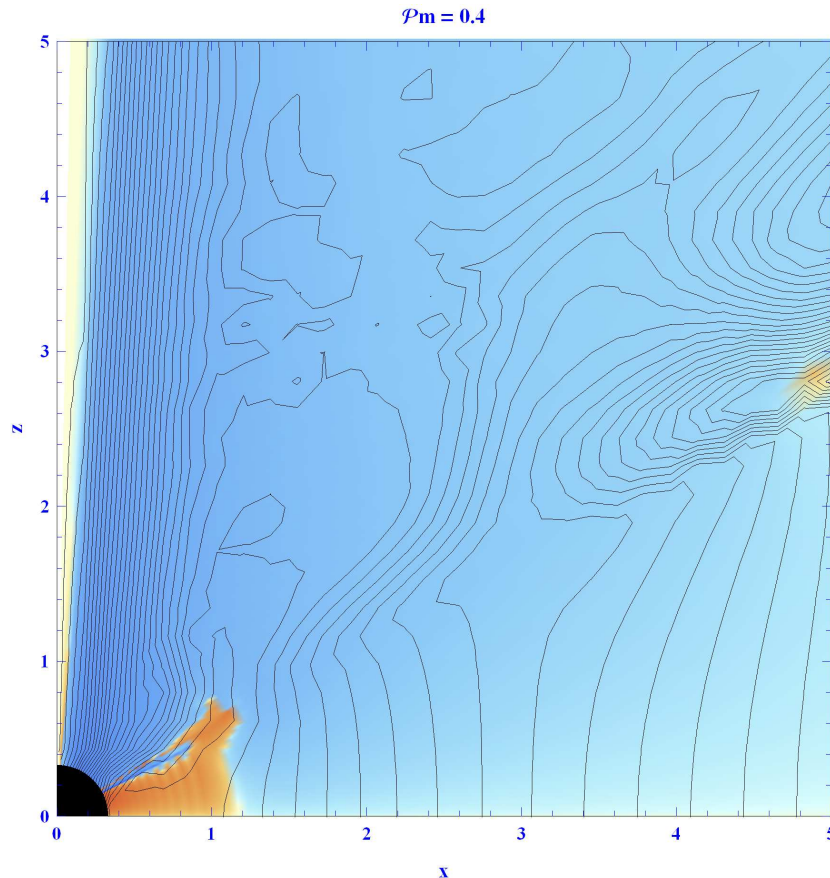


**Figure 5.** Configuration (f) of Fig. 1 ( $\mathcal{P}_m = 0.4, t = 38.4t_{\text{acc}}$ ) shown over a larger spatial scale. The central flux accumulation proceeds unimpeded. However, at larger distances, the disk develops complex dynamic magnetic activity.

$\eta$  case.

Our present realistic simulations of the Cosmic Battery at the inner edge of the accretion disk around a black hole confirm that this is an important astrophysical mechanism that may indeed account for the generation of the large scale magnetic field that threads astrophysical jets and disks. Under standard accretion disk conditions (magnetic Prandtl numbers of order unity), the Cosmic Battery generates a large scale magnetic field on the order of  $B_{\text{acc}} \sim 1$  G inside the ISCO of a ten solar mass black hole within about one accretion time on the order of a few milliseconds. Assuming that the black hole is accreting at about 1% of its Eddington rate, in order for the accumulated magnetic field to reach an equipartition value on the order of  $10^7$  G, one has to wait for about  $10^9$  accretion times, or equivalently for about  $t_{\text{eq}} \sim 10^7$  seconds (a few months). The above numbers obviously scale with mass as can be seen in Table 1.

We have shown that the Cosmic Battery does not increase the value of the magnetic field that threads the accretion disk. The magnetic field remains several orders of magnitude below equipartition, and does not inhibit the action of the MRI in the disk. Of course, as the magnitude of the accumulated field inside the ISCO approaches equipartition, the mechanism will saturate, and the accumulated field will probably escape outward through the disk due to magnetic Rayleigh-Taylor instabilities around its inner edge (Tchekhovskoy et al. 2010, Contopoulos & Papadopoulos in preparation). This is interesting because when that happens, one expects to also

see magnetically driven outflows (winds) from the disk. In other words, unless the accumulated field approaches equipartition around the inner edge of the disk (and thus becomes unstable to magnetic Rayleigh-Taylor instabilities), we do not expect to see any strong wind emanating from the disk. This is contrary to what is expected in the scenario where the magnetic field is brought in from large distances through the disk, and thus threads the disk and generates strong steady disk winds. It is interesting that, although the overall growth of the generated and accumulated magnetic flux proceeds as described above, the return field that threads the accretion disk at large distance beyond  $r_{\text{ISCO}}$  shows a very complex behavior that results from the interaction between the accretion flow, the force-free magnetosphere and the surface transition region (Fig. 5). Such dynamic behavior is a far cry from the smooth steady-state configurations obtained in old calculations of the disk-wind interaction. Our results may have implications for the variability observed in flaring XRBs where a strong radio jet appears only when the system transitions from the hard to the soft high state (Kylafis et al. 2012).

Similar complex variability is also observed in the numerical simulations of Parfrey et al. (2015) which are similar in concept to the ones presented in this work, although they solve only for the magnetospheric field. In the latter, the magnetic flux loops that inflate and open up are sustained by the disk turbulence as a boundary condition, and this is the reason highly variable reconnecting current sheets appear everywhere throughout

**Table 1**  
Timescales to reach equipartition

$M$	$B_{\text{acc}}$	$t_{\text{acc}}$	$B_{\text{eq}}$	$t_{\text{eq}}$
1	0.1	$10^{-3}$	$10^8$	one week
10	0.01	$10^{-2}$	$10^7$	a few months
$10^9$	$10^{-9}$	$10^6$	$10^3$	several Gyears

**Note.** —  $M$  (in solar masses): the mass of the central black hole;  $B_{\text{acc}}$  (in Gauss): the magnetic field accumulated inside the ISCO in one accretion time  $t_{\text{acc}}$  (in seconds);  $B_{\text{eq}}$  (in Gauss): the nominal equipartition magnetic field;  $t_{\text{eq}}$ : the time needed for the Cosmic Battery to build  $B_{\text{eq}}$ .

their simulations. Our physical picture differs in that we do account for the origin of a large scale magnetic flux of a well defined polarity that threads the disk and the inner compact object. In our case, only one reconnecting current sheet develops at the interface between outgoing and returning magnetic field lines.

Obviously, more investigation is required. Our work will be extended soon with general relativistic simulations that take into account the full distorted radiation field generated by the innermost hot accretion flow around the central spinning black hole (Koutsantonou & Contopoulos, in preparation).

This work was supported by the General Secretariat for Research and Technology of Greece and the European Social Fund in the framework of Action ‘Excellence’.

## REFERENCES

- Abramowicz, M. A. & Fragile, P. C., 2013, *Living Reviews in Relativity*, **16**, 1
- Abramowicz, M. A., Chen, X., Kato, S., Lasota, J. P., & Regev, O., 1995, *ApJ Lett.*, **438**, L37
- Balbus, S. A. & Hawley, J. F. 1991, *ApJ*, **376**, 214
- Biermann L., 1950, *Z.Naturforsch.*, **5a**, 65
- Bini, D., Jantzen, R. T. & Stella, L. 2009, *CQGra*, **26**, 5009
- Bisnovatyi-Kogan, G. S., Lovelace, R. V. E. & Belinski, V. A. 2002, *ApJ*, **580**, 380
- Blandford, R. D., 1993, in *Lighthouses of the Universe: The Most Luminous Celestial Objects and Their Use for Cosmology*, ed. M. Gilfanov, R. Sunyaev, & E. Churazov (Berlin: Springer), 381
- Blandford, R.D., 2002, in *Astrophysical Jets*, ed. D. Burgarella, M. Livio & C. P. O. O’Dea (Cambridge Univ. Press), 15
- Blandford, R. D. & Znajek, R. L. 1977, *MNRAS*, **179**, 433
- Cerutti, B., Philippov, A., Parfrey, K. & Spitkovsky, A. 2014, arXiv1410.3757
- Chen, X., Abramowicz, M. A., Lasota, J. P., Narayan, R. & Yi, I., 1995, *ApJ Lett.*, **443**, L61
- Christodoulou, D. M., Contopoulos, I. & Kazanas, D. 2008, *ApJ*, **674**, 388
- Contopoulos, I. 2013, *SoPh*, **282**, 419
- Contopoulos, I. & Kazanas, D. 1998, *ApJ*, **508**, 859
- Contopoulos, I., Kazanas, D. & Christodoulou, D.M., 2006, *ApJ*, **652**, 1451
- Contopoulos, Christodoulou, D.M., Kazanas, D. & Gabuzda, C., 2009, *ApJ Lett.*, **702**, L148
- Ferreira, J. & Pelletier, G. 1995, *A& A*, **295**, 807
- Gruzinov, A. 1999, arXiv/9902288
- Ho, L. C., *ARA&A*, **46**, 475
- Ichimaru, S. 1977, *ApJ*, **214**, 840
- Kalapotharakos, C. & Contopoulos, I. 2009, *A& A*, **496**, 495
- Komissarov, S. S., 2006, *MNRAS*, **368**, 993
- Koutsantonou, L. E. & Contopoulos, I. 2014, *ApJ*, **794**, 27
- Kylafis, N. D., Contopoulos, I., Kazanas, D. & Christodoulou, D. M. 2012, *A& A*, **538**, 5
- Lamb, F. K. & Miller, M. C. 1995, *ApJ*, **439**, 828
- Lasota, J. P., 1999, *Phys. Rep.*, **311**, 247
- Li, -Y 1995, *ApJ*, **444**, 848
- Lovelace R. V. E., Rothstein, D. M. & Bisnovatyi-Kogan, G. S., 2009, *ApJ*, **701**, 885
- Lynden-Bell, D. & Pringle, J. E., 1974, *MNRAS*, **168**, 603
- Murphy, E. & Gabuzda, D. 2013, in *The Innermost Regions of Relativistic Jets and their Magnetic Fields*, Ed. J. L. Gomez, EPJ, **61**, 7005
- Narayan, R. & Yi, I., 1994, *ApJ Lett.*, **428**, L13
- Narayan, R. & Yi, I., 1995a, *ApJ*, **444**, 231
- Narayan, R. & Yi, I., 1995b, *ApJ*, **452**, 710
- Narayan, R., Mahadevan R. & Quataert, E. 1998, in *Theory of Black Hole Accretion Disks*, ed. M.A. Abramowicz, G. Bjornsson & J.E. Pringle (Cambridge Univ. Press), 148
- Narayan, R. & McClintock, J. E. 2008, *New Astro. Rev.*, **51**, 733
- Nathanail, A. & Contopoulos, I. 2014, *ApJ*, **788**, 186
- Novikov, I. D., & Thorne, K.S., 1973, *Black holes (Les astres occlus)* 343-450
- Parfrey, K., Giannios, D. & Beloborodov, A. M. 2015, *MNRAS*, **446L**, 61
- Poynting, J. H. 1903, *MNRAS*, **64**, A1
- Quataert, E., 2001, in *Probing the Physics of Active Galactic Nuclei*, ed. B.M. Peterson, R.W. Pogge & R.S. Polidan, p. 71, San Francisco: ASP
- Rees, M. J., Begelman, M. C., Blandford, R. D. & Phinney, E.S., 1982, *Nature*, **295**, 17
- Reichstein, A. & Gabuzda, D. 2012, *JoP*, **355**, 2021
- Robertson, H. P. 1937, *MNRAS*, **97**, 423
- Shakura, N. I. & Sunyaev, R. A., 1973, *Astron. Astroph.*, **24**, 337
- Shapiro, S. L., Lightman, A. P. & Eardley, D. M., 1976, *ApJ*, **204**, 187
- Tchekhovskoy, A., Narayan, R. & McKinney, J. C. 2010, *ApJ*, **711**, 50
- Yuan, F. & Narayan, R., *ARA&A*, **52**, 529